

Control Volume Approach for Modeling the Interphase Mass Transfer in a Packed Column Distillation

Goro Nishimura¹, Kunio Kataoka¹, Hideo Noda¹ and Naoto Ohmura²

¹Kansai Chemical Engineering Co., Ltd., Amagasaki, Japan

²Department of Chemical Science and Engineering, Kobe University, Kobe, Japan

Abstract

A simplified mass transfer model for a ternary ideal solution was constructed by a control volume method proposed for a packed distillation column. The concept of modeling was in how to bridge between the distillation experiment of a real column and the computer-aided process simulation of an ideal column. The control volume approach using local values of HETPs determined by experiment was contrived to determine step-by-step local values of the vapor-phase and liquid-phase mass transfer coefficients. A commercial-scaled 5.5 m high packed column equipped with three beds of wire-mesh corrugated-structured packing was used as a test column. The experiment was conducted at normal pressure under the total-reflux condition for a ternary system of methanol, ethanol, and iso-propanol. The process simulation analysis for an ideal equilibrium-staged column was made to compare with the distillation experiment made by a real column. The volumetric film coefficients of mass transfer in the vapor phase and liquid phase, respectively, were evaluated step-by-step by the control volume method taking into account the experimentally obtained HETPs. Local variation of the experimental mass transfer correlations were generalized in a dimensionless form separating into the effect of local behavior and the Reynolds number dependency.

Keywords: Interphase mass transfer; Packed distillation column; Two film theory; Control volume method; Structured packing; total reflux operation

INTRODUCTION

There are two techniques available for modeling distillation [1]: the ideal stage (or equilibrium stage) model and the rate-based model. The rate-based model [2, 3, 4, 5], because of its very strict non-equilibrium concept, makes the theoretical approach possible by solving the differential transport equations but relies heavily on empirical correlation data of mass transfer coefficients. In addition, owing to the complicatedness of packed column distillation phenomena, there are not so many experimental investigations dealing with the interphase mass transfer. Some experimental studies [6, 7] are made on the vapor-phase mass transfer in a packed distillation column equipped with random packing. Their Sherwood number correlations are worthy to recognize from a viewpoint of the Reynolds number dependency. They try to compare the experimental data of diffusion-flux mass transfer coefficients between the two test columns: the 0.05 m high column and 0.50 m high column. However they do not analyze in detail the vertical variation of interphase mass transfer coefficients since their test columns were so small compared to a commercial scale packed column. There is no investigation elucidating local behavior of the interphase mass transfer in a commercial-sized packed column.

On the other hand, the ideal stage model is simple but very convenient to apply to various practical column design calculations. However the ideal stage model such as McCabe-Thiele model still remains to be improved for the experimental work on the interphase mass transfer in packed column distillation processes.

It is necessary to enrich the database of the interphase mass transfer correlations [8]. Owing to those circumstances, the purpose of this study is to observe local behavior of the interphase mass transfer in a real packed distillation column by collaborating with a computer-aided process simulation based on the equilibrium (or ideal) stage model. The previous study [9] tried to experimentally elucidate the F-factor dependency on local HETP (Height Equivalent to a Theoretical Plate) and HTU (Height of a Transfer Unit). The interest of the study was in the standardization of the HETP measurement conducted by the total reflux distillation experiment.

Correspondence to: Goro Nishimura, Kansai Chemical Engineering Co., Ltd., Amagasaki, Japan E-mail: nishimura@kce.co.jp

Received: May 16, 2021; **Accepted:** May 21, 2021; **Published:** June 1, 2021

Citation: Goro Nishimura (2021) Control Volume Approach for Modeling the Interphase Mass Transfer in a Packed Column Distillation. J Adv Chem Eng.11:195. doi: 10.35248/ 2090-4568.21.11.195

Copyright: © 2021 Goro Nishimura. This is an open-access article distributed under the terms of the Creative Commons Attribution License, which permits unrestricted use, distribution, and reproduction in any medium, provided the original author and source are credited.

According to Lockett's paper [10], the HETP decreases with the reboiler heat duty, and then seems to converge to a minimal value at 80% of the flooding point F-factor. Therefore only for simplification, all the distillation experiments in this study were also conducted under the total-reflux condition to determine local HETPs.

Their next study [11] tried to analyze a j-factor analogy between simultaneous heat and mass transfer in the same packed distillation column for a binary mixture. It has been confirmed that the binary distillation process in a structured packing column takes place accompanied with an analogy between the mass and enthalpy transfer in the vapor phase stream. The necessity of investigating local mass transfer behavior is emphasized especially for a commercial-scale packed column. Their analogy analysis [11] deals with length Reynolds number explaining the boundary-layer like development of simultaneous heat and mass transfer.

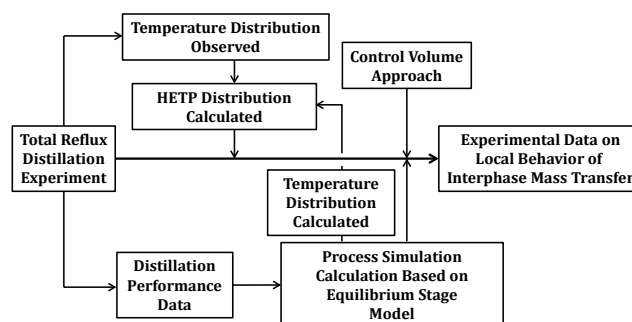


Figure 1: Interrelation between experiment and process simulation of packed column distillation and the flow diagram of data processing

Figure 1 indicates a flow diagram of the distillation experiment of a real packed column combined with the process simulation of an ideal column by a control volume approach for the data processing how to estimate local behavior of the interphase mass transfer. The process simulation calculation was conducted in the same condition taking into account the performance data obtained by the distillation experiment. Local HETPs were determined by comparing in liquid temperatures between the real column experiment and the ideal column calculation. After that, local coefficients of the interphase mass transfer can be estimated step-by-step applying the local HETPs to a control volume approach proposed in this study.

MODELING CONCEPT

The control volume approach [9, 11, 12] was employed for this experimental work to collaborate with the process simulation based on the equilibrium stage model, so that each control volume of a real column corresponds to each equilibrium stage of an ideal column.

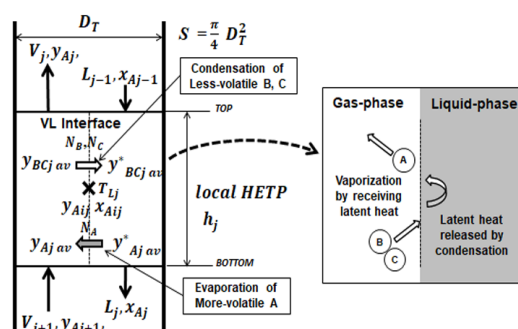


Figure 2: Definition of jth control volume in a packed column

Taking into account the local efficiency of distillation, each control volume defined in Figure 2 should have the corresponding local value of HETP as its height. As the j^{th} theoretical stage of an ideal column corresponds to the j^{th} control volume of a real packed column, the central

position of each control volume gives the equilibrium composition (y_{Aij}, x_{Aij}) at the vapor-liquid contacting interface of the temperature T_j .

At the same time, the bulk concentrations (y_{Aj}, x_{Aj}) of the vapor and liquid respectively leaving the control volume should also have the equilibrium relation: $y_{Aj} = K_A x_{Aj}$ because of an equilibrium stage. Similarly to the McCabe-Thiele method, as shown in Figure 3, the temperatures of the gas-phase T_{vj} , liquid-phase T_{lj} , and interface T_{ij} calculated on each equilibrium stage j are assigned step-by-step by the above control volume method.

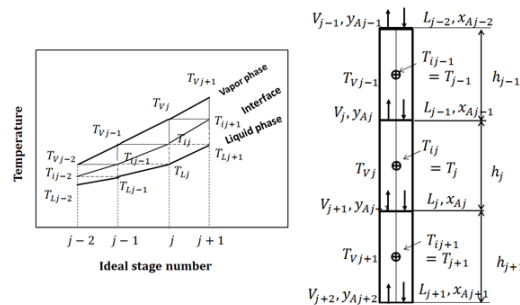


Figure 3: Step-by-step assignment of the calculated vapor-phase, liquid-phase, and interface temperatures into control volumes

By using the mass balance of the most volatile component A set up over the control volume of height h_j , two kinds of volumetric mass transfer coefficients $K_{yA}a$ and $k_{yA}a$ can be defined as

$$N_{Aj} = (K_{yA}a)_j \left[\left\{ (y_{Aj-1}^* - y_{Aj}) + (y_{Aj}^* - y_{Aj+1}) \right\} / 2 \right] h_j \quad (1)$$

$$N_{Aj} = (k_{yA}a)_j \{ y_{Aij} - (y_{Aj} + y_{Aj+1}) / 2 \} h_j \quad (2)$$

where the overall driving forces $y_A^* - y_A$ in Equation (1) are averaged between the top and bottom of the control volume. The y_A^* is the bulk concentration of the liquid phase converted into the units of the vapor-phase concentration. The top and bottom concentrations are averaged as the vapor bulk concentration y_{Aj} in Equation (2), where the first term y_{Aij} implies the interface equilibrium concentration equal to y_{Aj} given by the process simulation. It can be considered that local values of HETPs play a role of bridging between a real column and an ideal column.

The dividing ratio w is defined as the ratio of the vapor-phase driving force $y_{Aij} - y_{Abj}$ to the overall driving force $y_{Aj}^* - y_{Abj}$

$$w = \frac{y_{Aij} - y_{Abj}}{y_{Aj}^* - y_{Abj}} = \frac{K_{yA}}{k_{yA}} = \frac{1/k_{yA}}{1/K_{yA}} \quad (3)$$

This implies a ratio of the vapor-phase film resistance to the over-all resistance. Therefore the following relation can be deduced between the gas-phase and liquid-phase film coefficients:

$$(k_{xA}a)_j = \frac{w}{1-w} K_A (k_{yA}a)_j \quad (4)$$

where K_A is an equilibrium coefficient.

The control volume approach enables the determination of film coefficients of mass transfer $k_{yA}a$ and $k_{xA}a$ if local values of HETPs are obtained by the total-reflux distillation experiment with the aid of the process simulation based on the equilibrium stage model.

Process Simulation by Equilibrium-stage Model

A usual step-by-step process simulation based on the equilibrium stage model, which is similar to the McCabe-Thiele method, is performed under the total-reflux condition by the following set of mass and enthalpy balance equations [11] for an ideal mixture of m components:

(j^{th} stage of an ideal column)

$$M_{jk} = V_j y_{j,k} + L_j x_{j,k} - V_{j+1} y_{j+1,k} - L_{j-1} x_{j-1,k} = 0 \quad (5)$$

$$E_j = V_j H_{Gj} + L_j H_{Lj} - V_{j+1} H_{Gj+1} - L_{j-1} H_{Lj-1} = 0 \quad (6)$$

(Overhead condenser)

$$M_{1k} = L_1 x_{1,k} - V_2 y_{2,k} = 0 \quad (7)$$

$$Q_1 = L_1 H_{L1} - V_2 H_{G2} = 0 \quad (8)$$

(Bottom reboiler)

$$M_{Nk} = V_{Nk}y_{N,k} - L_{N-1}x_{N-1,k} = 0 \quad (9)$$

$$Q_N = V_N y_{N,k} - L_{N-1} x_{N-1,k} = 0 \quad (10)$$

(Equilibrium coefficient and equilibrium condition)

$$K_{j,k} = p_{k,sat}(T_j) / P \quad (11)$$

$$S_{j,k} = K_{j,k}x_{j,k} - y_{j,k} = 0 \quad (12)$$

(Mole fraction requirement)

$$X_j = \sum_{k=1}^m x_{j,k} - 1 = 0 \quad (13)$$

$$Y_j = \sum_{k=1}^m y_{j,k} - 1 = 0 \quad (14)$$

where the NRTL model is used to evaluate activity coefficients and physical properties of vapor and liquid of a ternary mixture ($m=3$).

A commercial process simulator package (PRO/II by ProSim) used in this study has the algorithm consisting of the above set of equations.

EXPERIMENTAL

Experimental method and apparatus

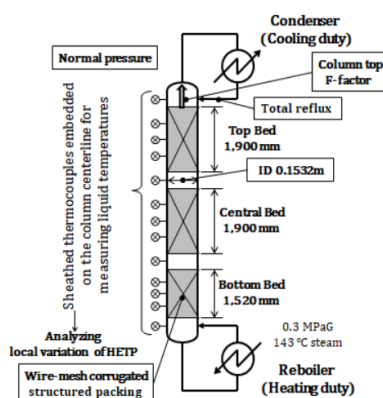


Figure 4: Experimental apparatus of a packed distillation column equipped with three beds of structured packing

Figure 4 shows an experimental packed distillation column [11] equipped with three beds of wire-mesh structured packing stacked up in series. They are 1.90 m, 1.90 m, and 1.52 m in bed height, respectively. The inside diameter of the column is $D_T = 0.1532$ m. The wire-mesh corrugated structured packing has the hydraulic equivalent diameter $d_{eq} = 0.00625$ m and the specific surface area $a_p = 500$ m^2/m^3 . Each empty space between those beds is equipped with a funnel-type liquid collector and a channel-type liquid distributor in order to avoid maldistribution of liquid stream.

In order to observe local variation of HETPs, nine sheathed thermocouples (1 mm OD) were embedded just on the column centerline at an equal interval (every 475 mm in the top and middle beds and every 380 mm in the bottom bed) in the packing section. It was assumed that those thermocouples could measure local liquid temperatures because of its large heat capacity. The distillation experiment was performed at normal pressure under the total-reflux condition by changing the heating duty of the bottom reboiler. In this experiment, the key component methanol (the most volatile component A) was kept high in concentration as compared with the remaining two components (component B: ethanol and component C: iso-propanol). The performance data obtained was used for the specification of the process simulation. In a usual way for the practical packed column design, the HETP measurement makes it a rule to conduct the total-reflux distillation test [10]. A ternary mixture of methanol, ethanol, and iso-propanol was adopted as the test system for assuming an ideal solution. The F-factors based on the superficial vapor velocity ($F = 0.5, 1.0, 1.5$, and 2 given in each figure) were evaluated at the column top position for specifying each experimental condition. Using those experimental performance data, the temperature and composition

profiles were calculated by using a commercial process simulator package (PRO/II by ProSim) based on the equilibrium stage model.

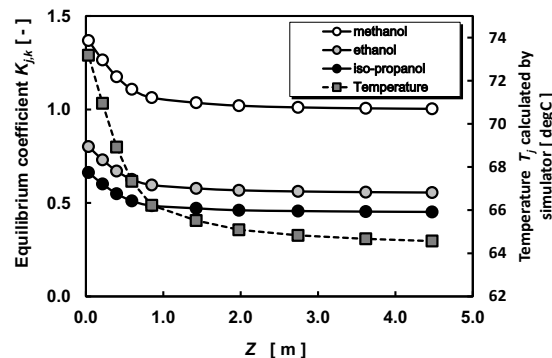


Figure 5: Local distribution of equilibrium coefficients of three components and temperature calculated by a process simulator ($F = 2.0$)

Figure 5 indicates the equilibrium coefficient $K_{j,k}$ for each component and liquid temperature T_j calculated by the process simulator when $F = 2.0$. The equilibrium coefficient of methanol is kept slightly larger than unity over the large part of the packing section in this experimental condition.

Determination of local HETPs

Local values of HETPs were evaluated by step-by-step comparing the theoretical temperature profiles T_n^{th} at theoretical stage n calculated for an ideal column with the experimental temperature profiles T_m^{ex} at a vertical position Z_m observed by the embedded thermocouples in a real column [11]. As shown in Figure 6, a local HETP is determined by the following equation:

$$h_j = \frac{T_n^{th} - T_{n-1}^{th}}{T_m^{ex} - T_{m+1}^{ex}} \times (Z_m - Z_{m-1}) \quad (15)$$

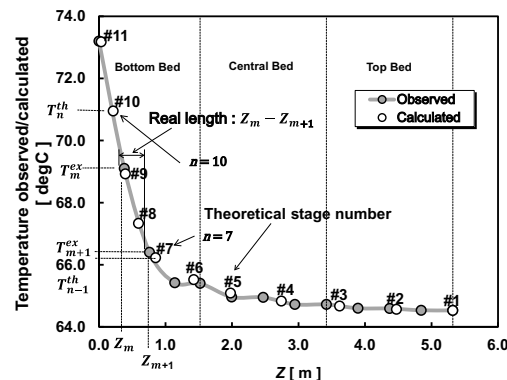


Figure 6: Determination of local HETPs by comparing the experimental temperature profiles with the theoretical temperature profiles calculated by a process simulator. ($F=2.0$)

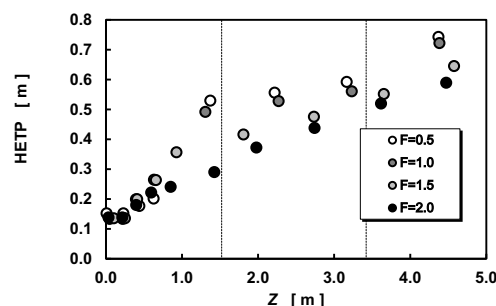


Figure 7: Vertical distribution of local HETPs experimentally obtained

Figure 7 indicates local distribution of HETPs obtained by experiment. It has been found that the HETPs become a minimal value at the lower edge (bottom) of the packing section and increase in the downstream direction of the vapor stream. This tendency implies that the distillation efficiency varies considerably over the whole region of the packing section. This also suggests the necessity of analyzing the mass transfer behavior from a viewpoint of local variation as well as the Reynolds number dependency.

EXPERIMENTAL RESULTS

Mass transfer distribution

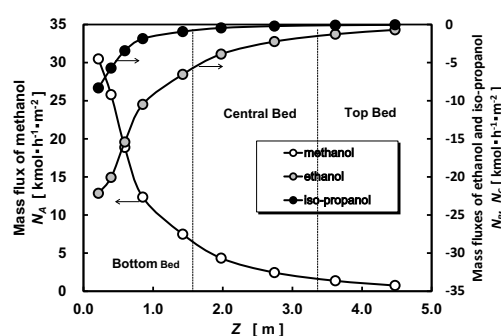


Figure 8: Vertical distribution of molar mass fluxes of three components obtained in the total-reflux condition ($F=2.0$)

Figure 8 shows the vertical distribution of molar mass-fluxes of the three components. The following mass-flux balance has been confirmed:

$$N_A + N_B + N_C = 0 \quad (16)$$

where the molar fluxes N_B and N_C are negative in the composition range adopted in the total-reflu distillation experiment.

This can be considered to be due to the equimolar counter-diffusion in the case of an ideal solution. Therefore the effect of partial condensation on the vapor-phase mass transfer [7] can be neglected for this simplified model.

From this viewpoint of interphase mass transfer, the distillation process should be distinguished from the gas absorption.

In this experimental composition range ($x_a \gg x_b \gg x_c$) of three components, the ethanol and iso-propanol components transfer together from the vapor bulk toward the interface for condensation while the methanol component vaporized in the liquid phase near the interface transfers in the opposite direction in the vapor stream.

$$N_A = -(N_B + N_C) \quad (17)$$

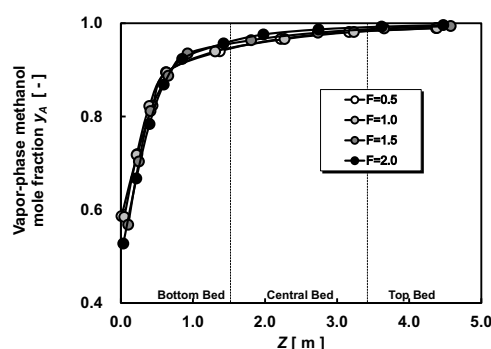


Figure 9: Vertical distribution of vapor-phase mole fractions of methanol component in a real column calculated from the composition profile for an ideal column

Figure 9 shows the vertical distribution of vapor-phase methanol composition for a real column calculated from the stage-by-stage composition profile of the process simulation results with the aid of the vertical distribution of HETPs experimentally obtained.

Local mass transfer coefficients

Local coefficients of the vapor-phase mass transfer in the j^{th} control volume were calculated for methanol component by the following equation:

$$N_{Aj} = V_j y_{Aj} - V_{j+1} y_{Aj+1} = (K_{yA} a)_j (y_A^* - y_A)_{j\text{av}} h_j = (k_{yA} a)_j (y_{Ai} - y_A)_{j\text{av}} h_j \quad (18)$$

where the concentration differences as the mass transfer driving force were averaged between the top and bottom of the control volume.

Similarly, local coefficients of the liquid-phase mass transfer of methanol were calculated by the following equation:

$$N_{Aj} = L_{j-1} x_{Aj-1} - L_j x_j = (K_{xA} a)_j (x_A - x_A^*)_{j\text{av}} h_j = (k_{xA} a)_j (x_A - x_{Ai})_{j\text{av}} h_j \quad (19)$$

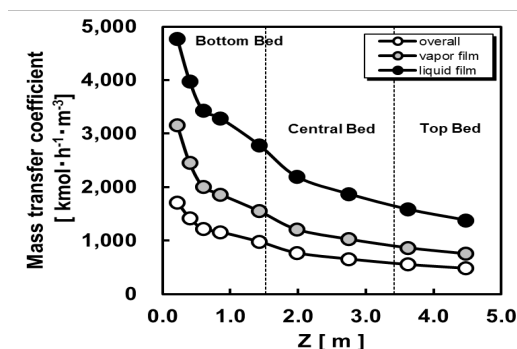


Figure 10: Vertical distribution of three kinds of volumetric mass transfer coefficients. ($F=2.0$)

Figures 10 indicates an example of calculated results: overall, vapor-phase film, and liquid-phase film coefficients of mass transfer. It has been confirmed that all the mass transfer coefficients become maximal near the lower edge (bottom) of the packing section and then decrease hyperbolically upward along the column height.

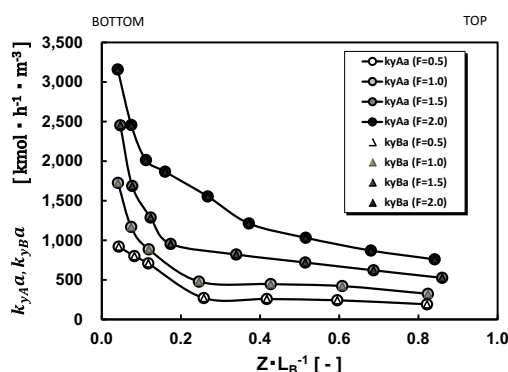


Figure 11: Vapor-phase mass transfer coefficients of methanol and ethanol ($F = 2.0$)

Figure 11 gives vertical distribution of vapor-phase mass transfer coefficients of methanol $k_{yA}a$ and ethanol k_{yBa} . The two kinds of mass transfer coefficients are always equal in magnitude to each other but opposite in the transfer direction. This is due to the fact that the ternary test mixture is a near-ideal solution.

This result can be explained with an assumption of an ideal solution as follows. The mass fluxes for a ternary ideal mixture are given by

$$N_A = k_{yA}a(y_{Ai} - y_{Ab})h_j \quad (20)$$

$$N_B = -k_{yB}a(y_{Bi} - y_{Bb})h_j \quad (21)$$

$$N_C = -k_{yC}a(y_{Ci} - y_{Cb})h_j \quad (22)$$

where the distillation condition in this study is assumed as

$$N_A + N_B + N_C = 0 \quad N_A > 0, N_B < 0, \text{ and } N_C < 0 \quad (23)$$

This indicates that the most volatile component A transfers from the vapor-liquid interface toward the vapor bulk whereas the remaining two components B and C transfer in the opposite direction in the vapor phase.

Because of a ternary system, Equation (22) can be rewritten as

$$N_C = -k_{yC}a[(y_{Bi} - y_{Bb}) + (y_{Ai} - y_{Ab})]h_j \quad (24)$$

Therefore the total mass flux of the component B and C becomes

$$N_B + N_C = -k_{yB}a(y_{Bb} - y_{Bi})h_j - k_{yC}a[(y_{Bi} - y_{Bb}) + (y_{Ai} - y_{Ab})]h_j \quad (25)$$

Finally assuming no effect of the partial condensation [7], the total molar fluxes can be written as

$$N_A + N_B + N_C = (k_{yA}a - k_{yC}a)(y_{Ai} - y_{Ab})h_j + (k_{yB}a - k_{yC}a)(y_{Bi} - y_{Bb})h_j = 0 \quad (26)$$

This equation should always hold good under the following requirement:

$$k_{xA}a = k_{xB}a = k_{xC}a \quad (\text{for a ternary ideal solution}) \quad (27)$$

Similarly the relation: $k_{xA}a = k_{xB}a = k_{xC}a$ can be obtained in the liquid-phase mass transfer.

Therefore the mass transfer data of methanol are principally given in the remaining part of the article.

Generalization of mass transfer correlations

In order to construct a simplified mass transfer model, it is a very important and useful way to generalize all the experimental and theoretical data in a dimensionless form by separating into the two parts: the local variation effect and the Reynolds number dependency.

The dimensionless groups are defined as

$$Sh_G = \frac{(k_{yA}a)d_{eq}}{a_p \rho_{mG} D_{GAB}} \quad \text{and} \quad Sh_L = \frac{(k_{xA}a)d_{eq}}{a_p \rho_{mL} D_{LAB}} \quad (28)$$

$$Re_G = \frac{\rho_G (u_{SG} - u_{SL}) d_{eq}}{\mu_G} \quad \text{and} \quad Re_L = \frac{\rho_L (u_{SG} - u_{SL}) d_{eq}}{\mu_L} \quad (29)$$

$$Sc_G = \frac{\mu_G}{\rho_G D_{GAB}} \quad \text{and} \quad Sc_L = \frac{\mu_L}{\rho_L D_{LAB}} \quad (30)$$

Therefore the functional form can be assumed as

$$Sh_G = a Re_G^b Sc_G^c f(\zeta) \quad \text{and} \quad Sh_L = a' Re_L^{b'} Sc_L^{c'} g(\zeta) \quad (31)$$

where the two distribution functions $f(\zeta)$ and $g(\zeta)$ be expressed by a dimensionless vertical position $\zeta = Z / d_{eq}$ from the lower edge (bottom) of the packing section in the upward direction.

Dimensionless correlation of local mass transfer behavior

Vapor-phase mass transfer correlation

(1) Distribution function

After trial-and-error calculations, as shown in Figure 12, the following hyperbolic function was obtained as the distribution function by a parameter fitting method as

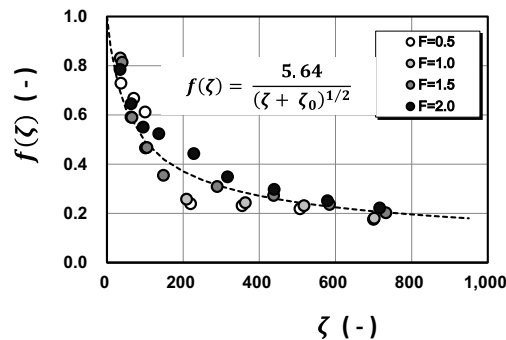


Figure 12: Distribution function for vapor-phase mass transfer coefficients ($\zeta_0 = 31.8$)

$$f(\zeta) = \frac{5.64}{(\zeta + \zeta_0)^{1/2}} \quad (32)$$

The term $\zeta_0 = 31.8$ implies that the virtual origin deviates by approximately $Z_0 = 0.20$ m on the downside from the lower edge of the packing section. It was not so easy to make the origin of vertical column height coincident with the bottom of the packing section. It is very difficult to make the lower edge of the packing section play a role of the leading edge of boundary layer development [11].

(2) Reynolds number dependency

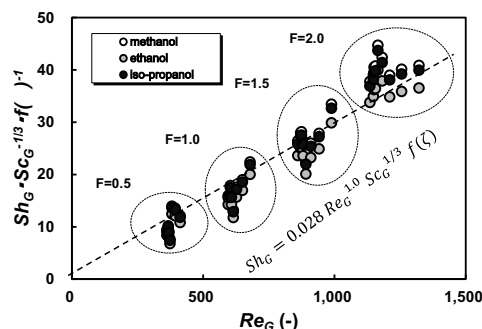


Figure 13: Variation of the vapor-phase Sherwood number with the vapor phase Reynolds number

As shown in Figure 13, the Reynolds number dependency was examined in the form of $Sh_G / Sc_G^{1/3} / f(\zeta)$ vs. Re_G

As a result, the mass transfer correlation of the vapor-phase film was settled down to the following form:

$$Sh_G = 0.028 Re_G^{1.0} Sc_G^{1/3} f(\zeta) \quad (33)$$

where the Schmidt number dependency is assumed as $c = 1/3$, similarly to j-factor definition [11].

The exponent of the Reynolds number $b = 1.0$ is coincident with the value assumed for random packings [8].

Liquid-phase mass transfer correlation

As distinct from the vapor-phase mass transfer, the liquid-phase mass transfer is considerably complicated because the liquid stream really flows down in the form of very complicated falling liquid film, which has solid walls of the packing as well as the vapor-liquid contacting interface. All the experimental data are somewhat more scattered.

(1) Distribution function

In a manner similar to the vapor-phase analysis, the liquid-phase correlation results obtained are given in Figures 14 and 15.

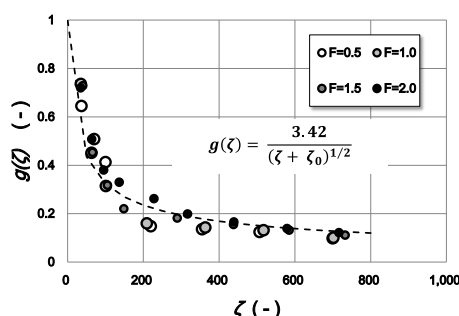


Figure 14: Distribution function of liquid-phase mass transfer ($\zeta_0 = 11.7$)

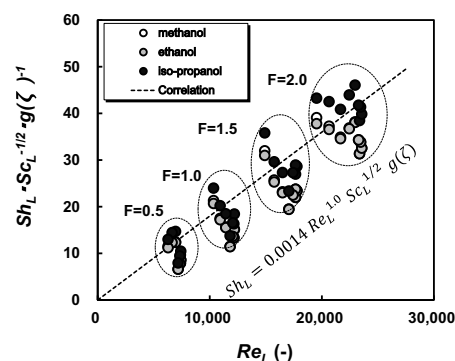


Figure 15: Variation of the liquid-phase Sherwood number with the liquid-phase Reynolds number

The distribution function for the liquid-phase mass transfer was also obtained in the same functional form as the vapor-phase one:

$$g(\zeta) = \frac{3.42}{(\zeta + \zeta_0)^{1/2}} \quad (34)$$

where ζ_0 implies that the origin of the vertical coordinate deviates by $\zeta_0 = 11.7$ ($Z_0 = 0.073$ m) on the downside from the bottom of the packing section.

(2) Reynolds number dependency

As shown in Figure 15, the Sherwood numbers for the liquid-phase mass transfer correlated with the Reynolds number were given by the following equation:

$$Sh_L = 0.0014 Re_L^{1.0} Sc_L^{1/2} g(\zeta) \quad (35)$$

The Schmidt number dependency of the liquid-phase correlation becomes different from the vapor-phase correlation but coincides with one of the assumed correlation [8].

DISCUSSION

Regarding the experimental investigations on the mass transfer in a packed distillation column, various data on the Reynolds number dependency are reported [6, 7, 13].

Two experimental studies [6, 7] investigate the vapor-phase mass transfer in the (random packing) packed column distillation of binary and ternary mixtures. They obtain the following correlations for the diffusion flux mass transfer by using the coefficient (J_{is} / N_i) for eliminating the effect of the convective mass flux:

$$Sh_G(J_{is} / N_i) = 0.0306 Re_G^{0.805} Sc_{Gis}^{1/3} G_v \quad (36)$$

where G_v is the function related with the partial condensation effect producing the convective mass flux.

Their vapor-phase Reynolds number for random packing is defined using a nominal size of packing as

$$Re_G = \frac{\rho_G u_{SG} D_p}{\mu_G} \quad (37)$$

Since the present study deals with a ternary mixture assumed as an ideal solution, it can be roughly assumed in their notation as:

$$(J_{is} / N_i) = 1 \quad \text{and} \quad G_v = 1$$

This implies the negligible effect of partial condensation [7]. Although their correlation for random packing [7] indicates a similar tendency, their exponent of the Reynolds number 0.805 differs a little bit from 1.0. However they did not discuss the local variation of mass transfer. They compare the experimental vapor-phase mass transfer correlations between two small test columns of 0.05 m and 0.5 m in height. They do not observe the liquid-phase mass transfer.

The mass transfer model for structured gauze packings is experimentally investigated to propose the practical design method [13]. They adapt the mass transfer correlation for counterflow in wetted-wall columns to the vapor-phase mass transfer in gauze packings. They obtain the following correlation [13]:

$$Sh_G = 0.0338 Re_G^{0.8} Sc_G^{0.333} \quad (38)$$

Their Sherwood number tendency is a little bit different from that of this study in the exponent of Reynolds number.

Regarding the liquid-phase mass transfer, they employ the penetration theory assuming the liquid stream as a falling liquid film flow and deduce the following correlation [13]:

$$k_L = 2 \left[D_L u_{L,eff} / (\pi S) \right]^{0.5} \quad (39)$$

This implies that $Sh_L \propto Re_L^{1/2}$. According to the film model, however, the correlation $Sh_L \propto Re_L^{1.0}$ is also assumed by [8].

On the other hand, the rate-based calculations for packed columns provide process engineers with a rigorous and reliable distillation basis and consideration but the rate-based simulation model has a serious weakness relying on empirical correlations for the mass transfer coefficients.

Regarding how to choose the right mass transfer correlations for the rate-based model, this problem [8] is dealt with in detail assuming the vapor-phase Sherwood number for random packings and structured packings respectively as

$$Sh_G \propto Re_G^1 Sc_G^{1/3} \quad (\text{random packings}) \quad (40)$$

This correlation equation coincides with the experimental results of this study in spite of different packings.

$$Sh_G \propto Re_G^1 Sc_G^{1/3} \left(\frac{\cos(\theta)}{\cos(\pi/4)} \right)^s \quad (\text{sheet metal corrugated structured packings}) \quad (41)$$

where the effect of inclination of corrugated structured packing is taken into account.

$$Sh_G \propto Re_G^{1/2} Sc_G^{1/3} \quad (\text{gauze structured packings}) \quad (42)$$

The Reynolds number dependency indicates an exponent different from that of this study because they assume the structured packing column to be similar to the wetted wall column.

These correlations still remain to be examined from a viewpoint of local behavior of interphase mass transfer.

At any rate, there are not many useful experimental data available on local variation of the interphase mass transfer in packed column distillation processes. Regarding the liquid-phase mass transfer, they assume the liquid-phase Sherwood number [8] for random and structured packings as

$$Sh_L \propto Re_L^1 Sc_L^{1/3} \quad (43)$$

This equation coincides in the Reynolds number dependency with that of this study.

Rate-controlling resistance of interphase mass transfer

The dividing ratio defined by Equation (3) indicates the ratio of the vapor-phase resistance to the overall mass transfer resistance.

$$w = \frac{y_{Aij} - y_{Abj}}{y_{Aj}^* - y_{Abj}} = \frac{1/k_{yA}}{1/K_{yA}} \quad (3)$$

This ratio can easily be evaluated by the control volume method.

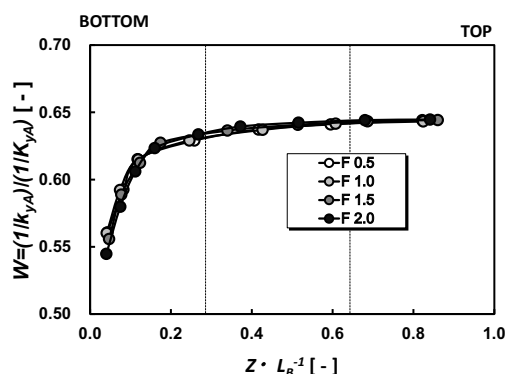


Figure 16: Variation of dividing ratio, i.e. the ratio of vapor-phase film resistance to the overall resistance of interphase mass transfer

As a result, Figure 16 indicates that the vapor-phase film resistance occupies approximately 65% of the overall resistance for the interphase mass transfer over the majority region of the packing section. Only in the vicinity of the lower edge (bottom) of the packing section where the mass flux becomes very large, the vapor-phase film resistance indicates lower than 65% but higher than 50%. It can be concluded that in the whole region of interphase mass transfer, the vapor-phase film plays a role of the rate-controlling resistance.

The method of practical packed column design should stand on the generalized dimensionless correlation equations separated into the Reynolds number dependency and the local variation effect when estimating the distillation efficiency of commercial-scale packed distillation columns. This correlation analysis is similar to the analogy analysis of boundary layer development [11, 12], which is also based on the control volume method proposed.

CONCLUDING REMARKS

A simplified model of methodology was constructed for local analysis of the interphase mass transfer in a structured packing column distillation. Considering that a general method of the practical packed column design should stand on the generalized dimensionless mass transfer correlations separated into the effect of local behavior and the Reynolds number dependency, the control volume method was contrived to bridge between the experimental analysis tested for a real packed column and the theoretical process simulation analysis based on the ideal equilibrium-stage model. A ternary mixture of methanol, ethanol, and iso-propanol was tested by the total-reflux distillation experiment. The vertical distribution of temperatures were measured by means of sheathed thermocouples embedded on the centerline of the test packed column and compared with the stage-by-stage temperature profiles calculated by the process simulator to determine the vertical distribution of HETPs.

The control volume method proposed has effectively deduced the vapor-phase and liquid-phase mass transfer correlations in a dimensionless form separating into two parts, the distribution function of local behavior and the Reynolds number dependency.

A simplified interphase mass transfer model of this kind is still required not only for the rate-based model but also for the practical design of packed distillation columns.

Nomenclature

- a = effective interfacial area
- a_p = specific surface area of packing
- D_{AB} = diffusivity
- d_{eq} = hydraulic equivalent diameter of packing
- D_p = nominal size of random packing
- D_T = inside diameter of a packed column
- F = F-factor based on superficial vapor velocity ($= u_{sG} \sqrt{\rho_G}$)
- f = distribution function of vapor-phase mass transfer coefficient
- g = distribution function of liquid-phase mass transfer coefficient

H	= molar enthalpy
h	= height of control volume (HETP)
HETP	= height equivalent to a theoretical plate
K_A	= equilibrium coefficient
k_x, k_y	= film coefficient of mass transfer, in liquid phase and vapor phase
K_x, K_y	= overall coefficient of mass transfer, defined by liquid concentration units and vapor concentration units
L	= superficial molar velocity of liquid
L_B	= total height of packing section
N	= molar mass flux
P, p	= total and partial pressures
Re	= Reynolds number
Sc	= Schmidt number
Sh	= Sherwood number
T	= temperature
u	= velocity
V	= superficial molar velocity of vapor
w	= dividing ratio defined by Equation (3)
x	= mole fraction of liquid
y	= mole fraction of vapor
Z	= vertical distance from bottom of packing section
ζ	= dimensionless vertical distance (= Z/d_{eq})
μ	= viscosity
ρ	= density

Subscripts

A, B, C	= three components of a ternary mixture (A: the most-volatile, C: the lowest-volatile)
b	= bulk fluid
G	= vapor phase
i	= vapor-liquid contacting interface
j	= stage number or control volume number
m	= molar
k	= component number
L	= liquid phase
m	= thermocouple number
n	= theoretical stage number
x, y	= liquid-phase or vapor-phase

REFERENCES

1. Taylor R, Krishna R, Kooijman H (2003) Real-world modeling of distillation. Chemical Engineering Progress (CEP). July:28-39.
2. Krishnamurthy R, Taylor R (1985a) A nonequilibrium stage model of multicomponent separation process I – Model description and method of solution. AIChE Journal. 31:449-456.
3. Krishnamurthy R, Taylor R (1985b) A nonequilibrium stage model of multicomponent separation process II – Comparison with Experiment. AIChE Journal 31:456-465.
4. Krishnamurthy R, Taylor R (1985c) A nonequilibrium stage model of multicomponent separation process III – The influence of unequal component-efficiency in process design problems. AIChE Journal 31:1973-1985.
5. Mori H, Oda A, Aragaki T (1996) Packed column distillation simulation with a rate-based method. Journal of Chemical Engineering of Japan 29:307-314.
6. Kosuge H, Matsudaira J, Aoki H, Asano K (1990) Experimental approach to mass transfer in binary packed column distillation. Journal of Chemical Engineering of Japan 23:593-599.
7. Kosuge H, Matsudaira J, Asano K (1991) Ternary mass transfer in packed distillation column. Journal of Chemical Engineering of Japan 24:455-460.
8. Hanley B, Chen C-C (2012) New mass-transfer correlations for packed towers. AIChE Journal 58:132-152.
9. Nishimura G, Kataoka K, Noda H, Yamaji H, Ohmura N (2020) Experimental study on mass transfer in a packed distillation column. Journal of Chemical Engineering of Japan 53:402-408.
10. Lockett MJ (1998) Easily predict structured-packing HETP. Chemical Engineering Progress (CEP) January:60-66.
11. Nishimura G, Kataoka K, Noda H, Ohmura N (2020) Computer-aided semi-empirical model of interphase mass and enthalpy transfer in a packed column distillation process. Proceedings 30th European Symposium on Computer Aided Process Engineering (ESCAPE30) 1-6.
12. Kataoka K (2021) Transport Process Chemical Engineering, <https://www.kce.co.jp/en/library/> Part II: 145-151.
13. Bravo JL, Rocha JA, Fair JR (1985) Mass transfer in gauze packings. Hydrocarbon Processing January:91-95.